Neuropathology and Cellular Pathogenesis of Spinocerebellar Ataxia Type 12

Elizabeth E. O'Hearn, MD[#1,2], **Hyon S. Hwang, MS**[#2], **Susan E. Holmes, PhD**[#2], **Dobrila D. Rudnicki, PhD**[2,4], **Daniel W. Chung, MS**[2], **Ana I. Seixas, PhD**[2,7], **Rachael L. Cohen, DVM**[2,4], **Christopher A. Ross, MD, PhD**[1,2,3,4], **John Q. Trojanowski, MD, PhD**[6], **Olga Pletnikova, MD**[5], **Juan C. Troncoso, MD**[1,5], and **Russell L. Margolis, MD**[1,2,4,*]

[1]Department of Neurology, Johns Hopkins University School of Medicine, Baltimore, Maryland, USA

[2]Laboratory of Genetic Neurobiology, Division of Neurobiology, Department of Psychiatry, Johns Hopkins University School of Medicine, Baltimore, Maryland, USA

[3]Departments of Neuroscience and Pharmacology, Johns Hopkins University School of Medicine, Baltimore, Maryland, USA

[4]Program in Cellular and Molecular Medicine, Johns Hopkins University School of Medicine, Baltimore, Maryland, USA

[5]Department of Pathology, Johns Hopkins University School of Medicine, Baltimore, Maryland, USA

[6]Institute on Aging, Alzheimer's Disease Core Center, Udall Parkinson's Research Center, Center for Neurodegenerative Disease, Department of Pathology and Laboratory Medicine, University of Pennsylvania School of Medicine, Philadelphia, Pennsylvania, USA

[7]Instituto de Biologia Molecular e Celular, Universidade do Porto, Oporto, Portugal

[#] These authors contributed equally to this work.

Abstract

Objective—SCA12 is a progressive autosomal-dominant disorder, caused by a CAG/CTG repeat expansion in *PPP2R2B* on chromosome 5q32, and characterized by tremor, gait ataxia, hyperreflexia, dysmetria, abnormal eye movements, anxiety, depression, and sometimes cognitive impairment. Neuroimaging has demonstrated cerebellar and cortical atrophy. We now present the neuropathology of the first autopsied SCA12 brain and utilize cell models to characterize potential mechanisms of SCA12 neurodegeneration.

[*]**Correspondence to:** Dr. Russell L. Margolis, Department of Psychiatry, Johns Hopkins University School of Medicine, CMSC 8-121, 600 North Wolfe Street, Baltimore, MD 21287, USA; rmargoli@jhmi.edu.

Methods—A fixed SCA12 brain was examined using gross, microscopic, and immunohistochemical methods. The effect of the repeat expansion on *PPP2R2B Bβ1* expression was examined in multiple cell types by transient transfection of constructs containing the *PPP2R2B Bβ1* promoter region attached to a luciferase reporter. The neurotoxic effect of *PPP2R2B* overexpression was examined in transfected rat primary neurons.

Results—Neuropathological investigation revealed enlarged ventricles, marked cerebral cortical atrophy and Purkinje cell loss, less-prominent cerebellar and pontine atrophy, and neuronal intranuclear ubiquitin-positive inclusions, consistent with Marinesco bodies, which did not stain for long polyglutamine tracts, alpha-synuclein, tau, or transactive response DNA-binding protein 43. Reporter assays demonstrated that the region of *PPP2R2B* containing the repeat functions as a promoter, and that promoter activity increases with longer repeat length and is dependent on cell type, repeat sequence, and sequence flanking the repeat. Overexpression of *PPP2R2B* in primary cortical neurons disrupted normal morphology.

Conclusions—SCA12 involves extensive, but selective, neurodegeneration distinct from Alzheimer's disease, synucleinopathies, tauopathies, and glutamine expansion diseases. SCA12 neuropathology may arise from the neurotoxic effect of repeat-expansion–induced overexpression of *PPP2R2B*.

Spinocerebellar ataxia type 12 (SCA12) is an autosomal-dominant disorder characterized by head and arm tremor, gait ataxia, hyperreflexia, dysmetria, abnormal eye movements, psychiatric disorders, and, in older patients, dementia.[1] MRIs of affected individuals reveal generalized atrophy of the brain, predominantly affecting the cerebral cortex and cerebellum.[2] Age of onset ranges from 8 to 55 years of age, but the disease usually presents in the fourth decade of life. The disease is most prevalent in India, where it is one of the most common forms of SCA in populations thus far sampled,[3-5] but it has also been identified in one American family of European descent[1] and a few European and non-Indian Asian families.[6-9] SCA12 is caused by a cytosine-adenine-guanine/cytosine thymine guanine (CAG/CTG) repeat expansion immediately flanking exon 7 on chromosome 5q32 in the gene for *PPP2R2B*.[10] Repeat length in the normal population ranges from 4 to 32 triplets, with a mode of 10 triplets in all populations sampled to date. Repeat length associated with disease ranges from 46 to 78 triplets; repeats of intermediate length and of uncertain significance have also been detected.[8,11] The multiple isoforms of *PPP2R2B* (Fig. 1) encode different *Bβ* regulatory units of the heterotrimer protein phosphatase 2A (PP2A). These regulatory units serve to direct PP2A toward specific targets, with specificity conferred by N-terminal sequence. Bioinformatic analysis at the time of mutation discovery indicated that the repeat, in the CAG orientation, was present 133 nucleotides upstream of the 5' end of the first exon of *PPP2R2B* (NM_004576; now NR_073526). Subsequent investigations identified six additional 5' exons, such that the exon associated with the repeat is now referred to as exon 7.[2] The predominant protein product, Bβ1, is encoded by a transcript that usually begins with exon 7. The CAG repeat appears to be largely untranscribed,[12] but does fall within the promoter region of the most common Bβ1-encoding transcripts.

The pathogenic pathways involved in SCA12 remain unknown. One possibility, based on the location of the repeat within a predicted *PPP2R2B* promoter,[10] is that repeat length may influence the expression level of the *PPP2R2B* isoform that encodes Bβ1,[14,15] a phenomenon also observed at other repeat loci.[16-22] Here, we describe, for the first time, neuropathology of an SCA12 brain, and we provide evidence that this neuropathology may derive from an effect of the SCA12 repeat expansion on Bβ1 expression.[10,23]

Materials and Methods

Neuropathology

The brain was fixed in 10% formalin. Paraffin block sections (10-μm) were stained with Cresyl violet (Nissl stain), hematoxylin and eosin (H & E), and silver by Hirano's method.[24] After deparaffinization, sections were immunostained for ubiquitin, expanded polyglutamine repeats (1C2 antibody[25]; see Supporting Table 1), glial fibrillary acidic protein (GFAP), synuclein-1, tau (PHF-1), and transactive response DNA-binding protein 43 (TDP-43). Sections were examined with an Olympus (Olympus, Tokyo, Japan) and a Leitz DMRB/E microscope and photographed with a Leica DC500 camera (Leica Microsystems GmbH, Wetzlar, Germany) (see Supporting Methods).

Plasmid Constructs

The pCAT-Basic reporter vector (Promega, Madison, WI) was used to create *PPP2R2B* plasmid constructs with repeat lengths of CAG_{10}, CAG_{24}, CAG_{35}, CAG_{53}, and CAG_{78}. A *Huntingtin* CAG_{80} construct and a C-G content of approximately 65% construct were generated. Luciferase constructs were then generated from the chloramphenicol acetyltransferase (CAT) constructs by removing the 1.7-kilobase (kb) promoter region and cloning into pGL3-Basic (luciferase vector; Promega) (Supporting Fig. 1).

Reporter Assay

LA-N-1, N2a, and SK-N-AS lines were maintained using standard conditions (see Supporting Methods). Primary cortical neurons for reporter assays were prepared from fetal rats at 16 days of gestation, as previously described.[26] Forty-eight hours after transfection, cells were harvested, lysed, and assayed for promoter activity. Luciferase activity was normalized to the internal control by calculating the ratio of firefly luciferase activity to Renilla luciferase activity of each sample. Normalized firefly luciferase activity for each test construct was expressed relative to expression of pGL3-Control plasmid (luciferase driven by an SV40 promoter). CAT activity, as corroboration for the luciferase reporter assay, was measured using pCAT-basic, pCAT-control, and experimental constructs in cells harvested 48 hours after transfection (Promega). At least three biological replicates were performed in triplicate for each experiment.

Transcript Expression

Total RNA was extracted from transfected LA-N-1 cells and complementary DNA (cDNA) was synthe-sized using random hexamers (see Supporting Methods). Real-time polymerase chain reaction (RT-PCR) was performed according to ABI protocols. Quantitative PCR (qPCR) assays were performed for firefly and Renilla luciferase and 18S RNA. For

assessment of transcript stability, LA-N-1 cells were transfected with *PPP2R2B*-CAG$_{10}$, -CAG$_{35}$, and -CAG$_{78}$ plasmids along with phRL-TK plasmid as internal control. Twenty-four hours after transfection, one set of cells were treated with 10 μg/mL of actinomycin D (ActD). Cells were harvested at 0, 1, 2, 3, and 6 hours after ActD treatment. Levels of luciferase messenger RNA (mRNA) were measured by qPCR.

Primary Cortical Neuron Toxicity Assay

Primary cortical neurons were transfected with *PPP2R2B*-pcDNA or empty pcDNA vector constructs using the Nucleofector system (Amaxa/Lonza, Cologne, Germany). The fragment of *PPP2R2B* expressed was *Bβ1* (exons 7 and 9–16; Fig. 1). Seventy-two hours after transfection, cells were fixed and stained with 1 μg/mL of Hoechst (Sigma-Aldrich, St. Louis, MO) in phosphate-buffered saline and mounted. Images were taken by fluorescence microscopy (Carl Zeiss, Thornwood, NY). Neurite complexity was evaluated quantitatively using Sholl analysis.[27] At least 40 neurons were counted per condition in each experiment. Three independent experiments were performed with embryos from different progenitors.

Results

Gross Neuropathology

The clinical description of the index family proband has been reported previously.[1] Genotyping revealed a 73 CAG triplet expansion in *PPP2R2B*.[10] In brief, she developed action tremor of both upper extremities in her thirties, followed by head tremor, gait ataxia, urinary incontinence, and cognitive decline over the next 30 years. Neurological exam at age 64 was notable for marked dementia, left-sided neglect, impersistence of movements, primitive reflexes, diffuse hyperreflexia with extensor plantar responses, paucity of spontaneous movement, and mild, generalized bradykinesia. She exhibited action tremor of arms and head, mild limb dysmetria, saccadic and dysmetric eye movements, and left arm apraxia. Her gait had cerebellar and parkinsonian features. She died from urosepsis at age 66. Gross brain pathology was remarkable for diffuse cortical atrophy, particularly in the parietal and posterior frontal lobes, with mild atrophy in multiple other regions, including the cerebellar folia (Table 1; Fig. 2).

Microscopic Neuropathology

Microscopic examination of the cerebral cortex revealed normal differentiation of gray and white matter with preservation of neuronal layers and cytoarchitectonics, with no apparent loss of any particular neuronal population or astrogliosis. Silver stains showed rare neuritic plaques in frontal and parietal cortex and a single neurofibrillary tangle in the subiculum. Immunostaining with antibodies against phosphorylated tau was negative. The cerebral white matter was unremarkable. Caudate, putamen, globus pallidus, hypothalamus, amygdala, and hippocampus were normal. There was mild focal gliosis in the dorsomedial thalamus. In the midbrain, the substantia nigra pars compacta (SNpc) showed a normal number of pigmented neurons, with minimal pigment incontinence and no Lewy bodies. In the pons, the locus ceruleus showed a normal number of well-pigmented neurons free of Lewy bodies or intranuclear inclusions. In the nuclei of the basis pontis and in the medulla, occasional degenerating neurons and axons were noted.

The three-layered neuronal pattern of cerebellar cortex was preserved without notable change in thickness. The deep cerebellar nuclei (fastigial, globosus, emboliform, and dentate) appeared normal in size and cytology (not shown). Moderate loss of Purkinje cells, greater than expected for age, was observed by H & E staining (Fig. 3A,B) in the vermis and cerebellar hemispheres and occurred in patches of up to approximately 10 cells. Occasional rounded swellings of the proximal Purkinje cell axon (torpedoes) were found in the cerebellar granule cell layer, indicative of injured Purkinje cells. Cerebellar white matter was mildly thinned. GFAP immunostaining did not reveal evidence of activated Bergmann glia in cerebellar cortex.

Inclusions

In the midbrain, no ubiquitin-positive inclusions were noted in neuronal cytoplasm, glial cells, astrocytes, microglia, or oligodendroglia. No ubiquitin-positive inclusions were observed in the striatum, thalamus, locus coeruleus, deep cerebellar nuclei, vestibular nuclei, hippocampus, pontine nuclei, or inferior olivary nuclei.

Ubiquitin immunostaining revealed large intranuclear inclusions in SNpc, consistent with Marinesco bodies,[28] observed in multiple neurons within any 40× field (Fig. 3G). Cytoplasmic inclusions were not present. Many SNpc neurons contained one to four inclusions (Fig. 3H), were round, ranging from 1 to 5 μm in diameter (Fig. 3G–I), and typically adjacent to nucleoli. Ubiquitin staining was darkest in the outer rim of the inclusion (Fig. 3G–I). SNpc neurons with inclusions appeared morphologically normal, with intact plasma membranes and no neuronal swelling, nuclear condensation, or apparent depigmentation. Some of these inclusions were also H & E positive, appearing as round eosinophilic structures readily distinguishable from nucleoli (Fig. 3I).

Eosinophilic and ubiquitin-immunostained inclusions were found in rare Purkinje cells (Fig. 3D,E). These inclusions were consistently intranuclear, single, round, 1 to 5 μm in diameter, and were adjacent but separate from nucleoli. Ubiquitin-positive inclusions in Purkinje cells were more densely stained, but lacked the rim of increased ubiquitin observed in SNpc inclusions. The few Purkinje cells that contained ubiquitin-positive inclusions appeared morphologically normal, with intact nuclear and plasma membranes. Ubiquitin immunostaining revealed very rare 1- to 2-μm ubiquitin-positive neuronal intranuclear inclusions in layer 3 of the motor cortex (Fig. 3F). Multiple inclusions were found within one nucleus (Fig. 3F).

Immunostaining for expanded polyglutamine tracts (Fig. 3I), alpha-synuclein, tau, and TDP-43 was negative.

The Repeat-Containing Region of *PPP2R2B* Functions as a Promoter

We used a dual-luciferase cell assay to characterize the putative promoter region of *Bβ1*, as well as the effect of the CAG repeat and flanking sequence on promoter activity (Supporting Fig. S1). In recognition of the inherent limitation of this approach to promoter analysis,[29] activity analysis was performed in four different cell types: LA-N-1 and SK-N-AS (human neuroblastoma); N2a (mouse neuroblastoma); and primary rat cortical neurons. Results of key experiments were confirmed using CAT assay (data not shown).

First, we confirmed the strong promoter activity of the *PPP2R2B* repeat region previously reported in human neuroblastoma lines.[15] In LA-N-1 (Fig. 4A), in which *PPP2R2B* expression has been previously demonstrated,[30] the *PPP2R2B* construct with CAG_{10}, the modal repeat length in the human population, functions as a strong promoter, comparable to an SV40 promoter. Nearly identical results were obtained using the CAT reporter assay system (data not shown). A similar effect was detected in primary cortical neurons (Fig. 4A), but not in N2a or SK-N-AS cells, suggesting cell-type specificity of promoter activity.

Reporter Activity Is Correlated With CAG Repeat Length

We next investigated the effect of different CAG repeat lengths on reporter activity. In addition to CAG_{10}, we examined CAG_{24} (upper range of normal repeat length), CAG_{35} (an intermediate range of unknown clinical significance), CAG_{53} (low end of the pathogenic range), and CAG_{78} (high end of the pathogenic range). In LA-N-1 cells (Fig. 4A), there was a strong correlation between repeat length and reporter expression, with CAG_{10} significantly different from CAG_{35}, CAG_{53}, and CAG_{78}. Similar results were observed using a CAT reporter assay (data not shown). These results are consistent with previous findings in these neuroblastoma cells.[15] The same effect of increasing repeat length on reporter activity was evident in primary cortical neurons (Fig. 4A), but not in N2a or SK-N-AS lines. These findings support our hypothesis that repeat length is correlated with promoter activity, including in untransformed neurons.

Sequence Specificity of the Effect of the Repeat Expansion

Preliminary evidence from insertion of A-T repeats in place of the *PPP2R2B* CAG repeat suggested that repeat sequence may be an important factor influencing the efficiency of the *PPP2R2B* promoter.[15] We therefore asked the more specific question of whether the effect of repeat expansions on reporter activity was sequence specific (e.g., can replacement of the CAG repeat with a random sequence of equal G-C content also increase reporter activity?). We inserted a 192-bp sequence from a fetal brain cDNA clone, with G-C content of approximately 65%, immediately 3' to the CAG_{10} repeat in the *PPP2R2B*-CAG_{10} construct, generating a total length equivalent to 74 CAG triplets. Reporter activity induced by the $CAG_{10}+(NNN)_{64}$ construct was equivalent to that induced by the *PPP2R2B*-CAG_{10} construct in LA-N-1 cells and rat primary cortical neurons (Fig. 4A) and was significantly less than activity induced by the CAG_{78} construct. Thus, increased reporter activity observed with expanded CAG repeats appears to be, at least partially, sequence specific.

The Effect of CAG Repeat Expansion Is Dependent on Flanking Sequence

To address the question of whether the sequence flanking the CAG repeat modulates reporter activity in our assay, we utilized the CAG_{80}-HD construct, whose insert was of similar length to that of the *PPP2R2B* construct (Supporting Fig 1). Reporter activity driven by this construct was minimal (Fig. 4A); activity was significantly less than the CAG_{10} construct and substantially less than the CAG_{78} construct in LA-N-1 cells, as well as primary rat cortical neurons. These results indicate that sequence context (regions flanking the repeat) is an important determinant of reporter expression. This is potentially related to the presence of cyclic 3',5'-adenosine monophosphate response element-binding protein (CREB)1 and

specificity protein 1 (Sp1) recognition sites in sequence flanking the repeat, previously shown to influence *PPP2R2B* expression.[15]

Reporter Activity Level Correlates With Transcript Level

Genomic analysis of *PPP2R2B* exon 7 suggests that the CAG repeat is occasionally included in transcripts (Fig. 1). We determined, by RT-PCR and sequencing of the product, that the transcripts expressed in our assay do include the repeat and flanking regions. We also determined that a 505-bp region of the transcript, beginning 28 bp 3' to the end repeat, is excised. Whereas reporter assays are typically interpreted to indicate the promoter strength of the attached sequence, the presence of the repeat within the transcript in our assay could also have influenced reporter activity by altering translational efficiency. We therefore used qPCR (designed against luciferase mRNA) to examine construct transcript levels in LA-N-1 cells (Supporting Fig. 2) transfected with constructs containing different CAG repeat lengths. The results show that transcript levels correlate with promoter activity, indicating that the primary effect of the repeat expansion is not at the level of translation. Transcript degradation (measured by qPCR in the presence and absence of ActD) does not appear to be accelerated by increasing repeat lengths in the luciferase assay (data not shown), providing additional evidence that greater luciferase activity with longer repeats reflects enhanced promoter activity.

Overexpression of *PPP2R2B* Reduces Neurite Outgrowth

To assess the potential impact of *PPP2R2B* overexpression on neurons, the predominate transcript, encoding Bβ1, was transfected into rat primary cortical neurons with the transfection marker, DsRed. Sholl analysis of transfected neurons revealed clear evidence of impaired neurite outgrowth, a marker of neuronal toxicity (Fig. 4B–D).[31]

Discussion

Here, we describe the first neuropathological study of an SCA12 brain. Gross examination revealed a small brain with generalized cerebral cortical atrophy, most prominently affecting the superior parietal and posterior frontal lobules bilaterally. The cerebellum and pons were mildly reduced in size. The ventricular system was moderately dilated throughout and the corpus callosum was abnormally thin, suggesting loss of commissural axons. Evidence of cell loss was not obvious in the cerebral cortex. Purkinje cell loss, but not granule cell loss, was readily apparent in the cerebellum. Ubiquitin immunoreactive, intraneuronal, intranuclear inclusions, consistent with Marinesco bodies, were abundant in SN neurons. Whereas Marinesco bodies are a common finding in the aged brain, they may be associated with motor dysfunction[28] and suggest possible SN dysfunction in this patient consistent with her parkinsonism. Similar appearing inclusions were found in rare Purkinje cells and in layer 3 neurons of prefrontal cortex. Inclusions were not detected in cytoplasm or glia. Inclusions did not stain with antibodies against long polyglutamine tracts, alpha-synuclein, tau, or TDP-43. Neuronal plaques and tangles were rare.

These findings demonstrate that SCA12 affects multiple brain regions, with changes most evident in the cerebral cortex and in the cerebellum, consistent with previous neuroimaging

results.[1,9] Pathology involves neuronal loss and, potentially, changes in the neuropil. This neuropathology is consistent with the main clinical features of the patient: action tremor, neglect, dementia, mild parkinsonism, and cerebellar dysfunction. Though many of the clinical and neurological findings observed in SCA12 are suggestive of multiple system atrophy (MSA), the neuropathological hallmarks of MSA, argyrophilic glial cytoplasmic inclusions staining for ubiquitin and synuclein,[32,33] were not detected. The absence of staining for long polyglutamine tracts also provides strong evidence that SCA12 is not a polyglutamine disease, particularly given that the repeat in this case, 73 triplets, is relatively long. The absence of detectable polyglutamine tracts is consistent with the infrequency with which the SCA12 repeat is transcribed. Even in rare transcripts containing the repeat (*Bβ7*, NM_181675), the repeat is in frame to encode serine rather than glutamine. In addition, neuropathological findings are not consistent with Alzheimer's disease, tauopathies, synucleinopathies, or frontotemporal lobar degeneration with ubiquitin-positive inclusions.[34]

The neuropathology reported here, in conjunction with previously reported neuroimaging and clinical findings,[1,9] demonstrates that SCA12 is quite distinct from other neurodegenerative diseases, including other SCAs, with practical implications for differential diagnosis and genetic testing of individuals presenting with an atypical neurodegenerative disorder. An important caveat is that the neuropathology findings reported here are from an individual with an expansion of 73 triplets, at the high end of the pathogenic range observed in SCA12, who had an unusually severe clinical course. It is therefore possible that the neuropathology in this individual is quantitatively or qualitatively different than individuals with more-modest repeat expansions. However, neuroimaging findings of other individuals with more modest expansions have also demonstrated atrophy in cortical and subcortical regions,[9] suggesting that SCA12, regardless of repeat length, is a diffuse disease not limited to the cerebellum.

The SCA12 repeat expansion may lead to SCA12 pathogenesis by multiple, nonmutually exclusive roles in regulation of *PPP2R2B* expression, as previously outlined for other repeat expansion diseases,[35,36] including RNA toxicity from transcripts containing the expanded repeat from either strand,[37,38] splicing dysregulation,[39] dysfunction of transcription or translation,[40-43] cryptic expression of a protein from a small open reading frame,[44] or repeat-associated non-ATG translation (RAN translation).[45] However, given the location of the SCA12 repeat immediately 5' to *PPP2R2B* exon 7, the first exon in the most common *PPP2R2B* transcript, we chose to test the hypothesis that the repeat expansion influences transcript expression.[40-42]

The results of our cell experiments, consistent with previous findings,[14,15] suggest that the SCA12 repeat locus, flanking and partially including exon 7, serves as a functional promoter, and that the strength of promoter activity increases with increasing CAG/CTG repeat length, so that repeats in the expanded range lead to marked increase in activity. In addition, the cell type, the sequence of the repeat itself, and the region flanking the repeat all are important features in promoter activity. Promoter activity, and the influence of repeat length, was detectable in one of three neuroblastoma lines, as well as in primary cortical neurons. This result is opposite to that observed in progressive myoclonus epilepsy type 1, in which expansion of a dodecamer repeat causes disease by reducing transcription.[46-48] The

effect of the SCA12 repeat expansion is similar to that observed in *FMR1*, with repeats of an intermediate length (56–200 triplets), which is associated with premature ovarian failure and the fragile X-associated tremor/ataxia syndrome. The mechanism by which these repeat expansion mutations influence promoter function remains to be determined, but presumably involves quantitative or qualitative changes in binding efficiency of transcription factors at the promoter locus.[49]

The conclusion that the SCA12 repeat expansion increases expression of the *PPP2R2B* isoform encoding Bβ1 must be tempered by the complex alternative splicing of *PPP2R2B*, and the likelihood that *PPP2R2B* expression is regulated by multiple promoters, each with their own complex regulation. For instance, CREB1 and SP1 binding 5' of the *PPP2R2B* exon 7 repeat upregulate *PPP2R2B* expression, whereas TFAP4, binding 3' to the repeat, downregulates *PPP2R2B* expression.[15] It is possible that within the full-length *PPP2R2B* gene, or within other cell types or at different stages of cell development, repeat length might have a different or additional effect on gene expression, such as an influence on splicing. The availability of only a single fixed SCA12 brain, and the lack of *PPP2R2B* expression in lymphoblastoid lines, has limited the ability to compare the levels of *PPP2R2B* variants in SCA12 patients with controls. Future availability of brain or biopsy tissue, particularly the generation of induced pluripotent stem (iPS) cells with the *PPP2R2B* expansion, may help validate the predictions of our model.

The findings in our study have potential pathogenic implications for SCA12. *PPP2R2B* is one of 18 known genes encoding PP2A-regulatory subunits.[12,50,51] *PPP2R2B* encodes a brain-specific regulatory subunit, Bβ (also termed PR55β), of PP2A, a ubiquitous serine/threonine phosphatase implicated in numerous normal and abnormal cellular processes, including apoptosis and tau phosphorylation.[30,52] PP2A is a heterotrimer with a structural, catalytic, and a regulatory B subunit.[53] The multiplicity of available B subunits results in dozens of different PP2A holoenzyme possibilities, with B subunits providing key information for differential substrate specificity, subcellular targeting, and PP2A enzyme kinetics.[52,54-56] *PPP2R2B* is spliced to encode multiple different protein isoforms, Bβ_n, which differ at their N-termini, the region that provides targeting information for the PP2A holoenzyme.[55] Increased activity of the exon 7–associated promoter would presumably increase levels of isoform *Bβ1*, potentially offsetting the normal decline in Bβ1 observed (in the rat) during normal postnatal development.[54,55] We speculate that overexpression of Bβ1 may shift the normal ratio of regulatory subunits forming the PP2A complex, resulting in a quantitative shift in PP2A targeting with eventual neurotoxic effects. Given that overexpression of Bβ1 in PC12 cells does not lead to marked changes in cell viability,[55] it is possible that Bβ1-associated neurotoxicity is a slow or cell-specific process or involves properties such as neurite outgrowth more prominently than cell loss. Overexpression of Bβ2 causes mitochondrial fragmentation leading to apoptosis in transgenic *Drosophila*,[57] as well as neuroblastoma and primary hippocampal neurons,[58] confirming the potential cytotoxicity of relative or absolute excess expression of *PPP2R2B* isoforms. Future cell and mammalian models, including the generation of SCA12 iPS cells, may lead to illumination of this and other mechanisms of pathogenesis.

Supplementary Material

Refer to Web version on PubMed Central for supplementary material.

Acknowledgments

References

1. O'Hearn E, Holmes SE, Calvert PC, et al. SCA-12: tremor with cerebellar and cortical atrophy is associated with a CAG repeat expansion. Neurology. 2001; 56:299–303. [PubMed: 11171892]

2. O'Hearn E, Holmes SE, Margolis RL. Spinocerebellar ataxia type 12. Handb Clin Neurol. 2012; 103:535–547. [PubMed: 21827912]

3. Bahl S, Virdi K, Mittal U, et al. Evidence of a common founder for SCA12 in the indian population. Ann Hum Genet. 2005; 69:528–534. [PubMed: 16138911]

4. Fujigasaki H, Verma IC, Camuzat A, et al. SCA12 is a rare locus for autosomal dominant cerebellar ataxia: a study of an indian family. Ann Neurol. 2001; 49:117–121. [PubMed: 11198281]

5. Srivastava AK, Choudhry S, Gopinath MS, et al. Molecular and clinical correlation in five indian families with spinocerebellar ataxia 12. Ann Neurol. 2001; 50:796–800. [PubMed: 11761478]

6. Brussino A, Graziano C, Giobbe D, et al. Spinocerebellar ataxia type 12 identified in two italian families may mimic sporadic ataxia. Mov Disord. 2010; 25:1269–1273. [PubMed: 20629122]

7. Zhao Y, Tan EK, Law HY, et al. Prevalence and ethnic differences of autosomal-dominant cerebellar ataxia in Singapore. Clin Genet. 2002; 62:478–481. [PubMed: 12485197]

8. Dong Y, Wu JJ, Wu ZY. Identification of 46 CAG repeats within PPP2R2B as probably the shortest pathogenic allele for SCA12. Parkinsonism Relat Disord. 2015; 21:398–401. [PubMed: 25634432]

9. Li H, Ma J, Zhang X. Diffusion tensor imaging of spinocerebellar ataxia type 12. Med Sci Monit. 2014; 20:1783–1791. [PubMed: 25274186]

10. Holmes SE, O'Hearn EE, McInnis MG, et al. Expansion of a novel CAG trinucleotide repeat in the 5' region of PPP2R2B is associated with SCA12. Nat Genet. 1999; 23:391–392. [PubMed: 10581021]

11. Musova Z, Sedlacek Z, Mazanec R, et al. Spinocerebellar ataxias type 8, 12, and 17 and dentatorubro-pallidoluysian atrophy in czech ataxic patients. Cerebellum. 2013; 12:155–161. [PubMed: 22872568]

12. Holmes, SE.; O'Hearn, E.; Cortez-Apreza, N. Spinocerebellar Ataxia 12 (SCA12). Elsevier Academic; San Diego, CA: 2006.

13. Ince TA, Scotto KW. A conserved downstream element defines a new class of RNA polymerase II promoters. J Biol Chem. 1995; 270:30249–30252. [PubMed: 8530439]

14. Chen CM, Hou YT, Liu JY, et al. PPP2R2B CAG repeat length in the Han Chinese in Taiwan: association analyses in neurological and psychiatric disorders and potential functional implications. Am J Med Genet B Neuropsychiatr Genet. 2009; 150B:124–129. [PubMed: 18484086]

15. Lin CH, Chen CM, Hou YT, et al. The CAG repeat in SCA12 functions as a cis element to up-regulate PPP2R2B expression. Hum Genet. 2010; 128:205–212. [PubMed: 20533062]

16. Gebhardt F, Zanker KS, Brandt B. Modulation of epidermal growth factor receptor gene transcription by a polymorphic dinucleotide repeat in intron 1. J Biol Chem. 1999; 274:13176–13180. [PubMed: 10224073]

17. Itokawa M, Yamada K, Yoshitsugu K, et al. A microsatellite repeat in the promoter of the N-methyl-D-aspartate receptor 2A subunit (GRIN2A) gene suppresses transcriptional activity and correlates with chronic outcome in schizophrenia. Pharmacogenetics. 2003; 13:271–278. [PubMed: 12724619]

18. Iwashita S, Koyama K, Nakamura Y. VNTR sequence on human chromosome 11p15 that affects transcriptional activity. J Hum Genet. 2001; 46:717–721. [PubMed: 11776385]

19. Syagailo YV, Okladnova O, Reimer E, et al. Structural and functional characterization of the human PAX7 5'-flanking regulatory region. Gene. 2002; 294:259–268. [PubMed: 12234688]

20. Shimajiri S, Arima N, Tanimoto A, et al. Shortened microsatellite d(CA)21 sequence down-regulates promoter activity of matrix metalloproteinase 9 gene. FEBS Lett. 1999; 455:70–74. [PubMed: 10428474]

21. Yamada N, Yamaya M, Okinaga S, et al. Microsatellite polymorphism in the heme oxygenase-1 gene promoter is associated with susceptibility to emphysema. Am J Hum Genet. 2000; 66:187–195. [PubMed: 10631150]

22. Wang L, Soria JC, Chang YS, et al. Association of a functional tandem repeats in the downstream of human telomerase gene and lung cancer. Oncogene. 2003; 22:7123–7129. [PubMed: 14562040]

23. Holmes SE, Hearn EO, Ross CA, Margolis RL. SCA12: an unusual mutation leads to an unusual spinocerebellar ataxia. Brain Res Bull. 2001; 56:397–403. [PubMed: 11719278]

24. Yamamoto T, Hirano A. A comparative study of modified bielschowsky, bodian and thioflavin S stains on Alzheimer's neurofibrillary tangles. Neuropathol Appl Neurobiol. 1986; 12:3–9. [PubMed: 2422580]

25. Trottier Y, Lutz Y, Stevanin G, et al. Polyglutamine expansion as a pathological epitope in Huntington's disease and four dominant cerebellar ataxias. Nature. 1995; 378:403–406. [PubMed: 7477379]

26. Pletnikov MV, Ayhan Y, Xu Y, et al. Enlargement of the lateral ventricles in mutant DISC1 transgenic mice. Mol Psychiatry. 2008; 13:115. [PubMed: 18202691]

27. Sholl DA. Dendritic organization in the neurons of the visual and motor cortices of the cat. J Anat. 1953; 87:387–406. [PubMed: 13117757]

28. Beach TG, Walker DG, Sue LI, et al. Substantia nigra Marinesco bodies are associated with decreased striatal expression of dopaminergic markers. J Neuropathol Exp Neurol. 2004; 63:329–337. [PubMed: 15099023]

29. Cirulli ET, Goldstein DB. In vitro assays fail to predict in vivo effects of regulatory polymorphisms. Hum Mol Genet. 2007; 16:1931–1939. [PubMed: 17566082]

30. Mayer RE, Hendrix P, Cron P, et al. Structure of the 55-kDa regulatory subunit of protein phosphatase 2A: Evidence for a neuronal-specific isoform. Biochemistry. 1991; 30:3589–3597. [PubMed: 1849734]

31. Radio NM, Mundy WR. Developmental neurotoxicity testing in vitro: Models for assessing chemical effects on neurite outgrowth. Neurotoxicology. 2008; 29:361–376. [PubMed: 18403021]

32. Papp MI, Kahn JE, Lantos PL. Glial cytoplasmic inclusions in the CNS of patients with multiple system atrophy (striatonigral degeneration, olivopontocerebellar atrophy and Shy-Drager syndrome). J Neurol Sci. 1989; 94:79–100. [PubMed: 2559165]

33. Dickson DW, Lin W, Liu WK, Yen SH. Multiple system atrophy: a sporadic synucleinopathy. Brain Pathol. 1999; 9:721–732. [PubMed: 10517510]

34. Uryu K, Nakashima-Yasuda H, Forman MS, et al. Concomitant TAR-DNA-binding protein 43 pathology is present in Alzheimer disease and corticobasal degeneration but not in other tauopathies. J Neuropathol Exp Neurol. 2008; 67:555–564. [PubMed: 18520774]

35. Rudnicki DD, Margolis RL. Repeat expansion and autosomal dominant neurodegenerative disorders: consensus and controversy. Expert Rev Mol Med. 2003; 5:1–24.

36. Rudnicki DD, Margolis RL, Pearson CE, Krzyzosiak WJ. Diced triplets expose neurons to RISC. PLoS Genet. 2012; 8:e1002545. [PubMed: 22383898]

37. Rudnicki DD, Holmes SE, Lin MW, et al. Huntington's disease-like 2 is associated with CUG repeat-containing RNA foci. Ann Neurol. 2007; 61:272–282. [PubMed: 17387722]

38. Li LB, Yu Z, Teng X, Bonini NM. RNA toxicity is a component of ataxin-3 degeneration in drosophila. Nature. 2008; 453:1107–1111. [PubMed: 18449188]

39. Kanadia RN, Shin J, Yuan Y, et al. Reversal of RNA missplicing and myotonia after muscleblind overexpression in a mouse poly(-CUG) model for myotonic dystrophy. Proc Natl Acad Sci U S A. 2006; 103:11748–11753. [PubMed: 16864772]

40. Kenneson A, Zhang F, Hagedorn CH, Warren ST. Reduced FMRP and increased FMR1 transcription is proportionally associated with CGG repeat number in intermediate-length and premutation carriers. Hum Mol Genet. 2001; 10:1449–1454. [PubMed: 11448936]

41. Oostra BA, Willemsen R. A fragile balance: FMR1 expression levels. Hum Mol Genet. 2003; 12:R249–57. Spec No 2. [PubMed: 12952862]

42. Tassone F, Beilina A, Carosi C, et al. Elevated FMR1 mRNA in premutation carriers is due to increased transcription. RNA. 2007; 13:555–562. [PubMed: 17283214]

43. Chutake YK, Costello WN, Lam C, Bidichandani SI. Altered nucleosome positioning at the transcription start site and deficient transcriptional initiation in friedreich ataxia. J Biol Chem. 2014; 289:15194–15202. [PubMed: 24737321]

44. Wilburn B, Rudnicki DD, Zhao J, et al. An antisense CAG repeat transcript at JPH3 locus mediates expanded polyglutamine protein toxicity in Huntington's disease-like 2 mice. Neuron. 2011; 70:427–440. [PubMed: 21555070]

45. Zu T, Gibbens B, Doty NS, et al. Non-ATG-initiated translation directed by microsatellite expansions. Proc Natl Acad Sci U S A. 2011; 108:260–265. [PubMed: 21173221]

46. Alakurtti K, Virtaneva K, Joensuu T, et al. Characterization of the cystatin B gene promoter harboring the dodecamer repeat expanded in progressive myoclonus epilepsy, EPM1. Gene. 2000; 242:65–73. [PubMed: 10721698]

47. Lalioti MD, Antonarakis SE, Scott HS. The epilepsy, the protease inhibitor and the dodecamer: progressive myoclonus epilepsy, cystatin b and a 12-mer repeat expansion. Cytogenet Genome Res. 2003; 100:213–223. [PubMed: 14526183]

48. Lalioti MD, Scott HS, Buresi C, et al. Dodecamer repeat expansion in cystatin B gene in progressive myoclonus epilepsy. Nature. 1997; 386:847–851. [PubMed: 9126745]

49. Lalioti MD, Scott HS, Antonarakis SE. Altered spacing of promoter elements due to the dodecamer repeat expansion contributes to reduced expression of the cystatin B gene in EPM1. Hum Mol Genet. 1999; 8:1791–1798. [PubMed: 10441345]

50. Holmes SE, O'Hearn E, Margolis RL. Why is SCA12 different from other SCAs? Cytogenet Genome Res. 2003; 100:189–197. [PubMed: 14526180]

51. Schild A, Schmidt K, Lim YA, et al. Altered levels of PP2A regulatory B/PR55 isoforms indicate role in neuronal differentiation. Int J Dev Neurosci. 2006; 24:437–443. [PubMed: 17045446]

52. Janssens V, Longin S, Goris J. PP2A holoenzyme assembly: in cauda venenum (the sting is in the tail). Trends Biochem Sci. 2008; 33:113–121. [PubMed: 18291659]

53. Strack S, Ruediger R, Walter G, et al. Protein phosphatase 2A holoenzyme assembly: identification of contacts between B-family regulatory and scaffolding A subunits. J Biol Chem. 2002; 277:20750–20755. [PubMed: 11929880]

54. Strack S, Zaucha JA, Ebner FF, et al. Brain protein phosphatase 2A: developmental regulation and distinct cellular and subcellular localization by B subunits. J Comp Neurol. 1998; 392:515–527. [PubMed: 9514514]

55. Dagda RK, Zaucha JA, Wadzinski BE, Strack S. A developmentally regulated, neuron-specific splice variant of the variable subunit bbeta targets protein phosphatase 2A to mitochondria and modulates apoptosis. J Biol Chem. 2003; 278:24976–24985. [PubMed: 12716901]

56. Mumby M. The 3D structure of protein phosphatase 2A: new insights into a ubiquitous regulator of cell signaling. ACS Chem Biol. 2007; 2:99–103. [PubMed: 17313179]

57. Wang YC, Lee CM, Lee LC, et al. Mitochondrial dysfunction and oxidative stress contribute to the pathogenesis of spinocerebellar ataxia type 12 (SCA12). J Biol Chem. 2011; 286:21742–21754. [PubMed: 21471219]

58. Dagda RK, Merrill RA, Cribbs JT, et al. The spinocerebellar ataxia 12 gene product and protein phosphatase 2A regulatory subunit Bbeta2 antagonizes neuronal survival by promoting mitochondrial fission. J Biol Chem. 2008; 283:36241–36248. [PubMed: 18940801]
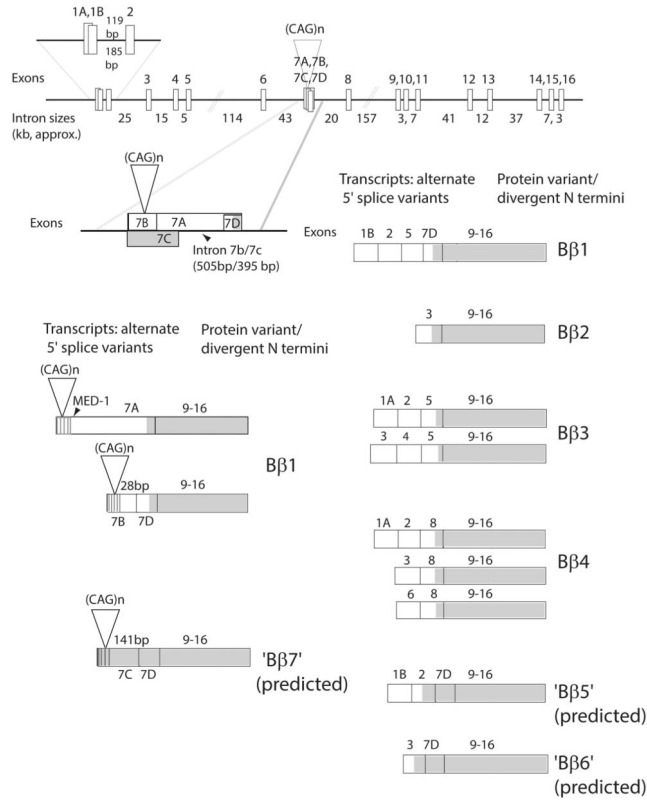
FIG. 1.

PPP2R2B structure and transcription expression. Exons are not to scale. The length of each intron is indicated in kb. Total gene length is approximately 493 kb. Alternate transcripts and their encoded proteins are depicted. Shaded regions of transcripts indicate open reading frames. The predominant transcript begins at exon 7 and encodes Bβ1. The predominant initiation site for transcripts beginning with exon 7 appears to be 3' to the repeat, with much less frequently used start sites 5' to the repeat and within the repeat. Exon 7 includes a multiply spliced internal intron (IVS 7b/7c) and a MED-1 (multiple start-site element downstream 1) sequence (GCTCCC)[13] 65 bp 3' to the CAG repeat.[10] Intron 7b/7c has two alternate donor sites (28 and 141 bp downstream from the repeat) spliced to a common acceptor site (127 bp upstream from the Bβ1 coding region). Use of the second donor site yields a transcript predicted to encode an alternate N-terminus in which the repeat encodes polyserine. Multiple combinations of upstream exons lead to protein variants with divergent N-termini; Bβ5-7 remain hypothetical. Edited and reprinted with permission from Elsevier.[12]
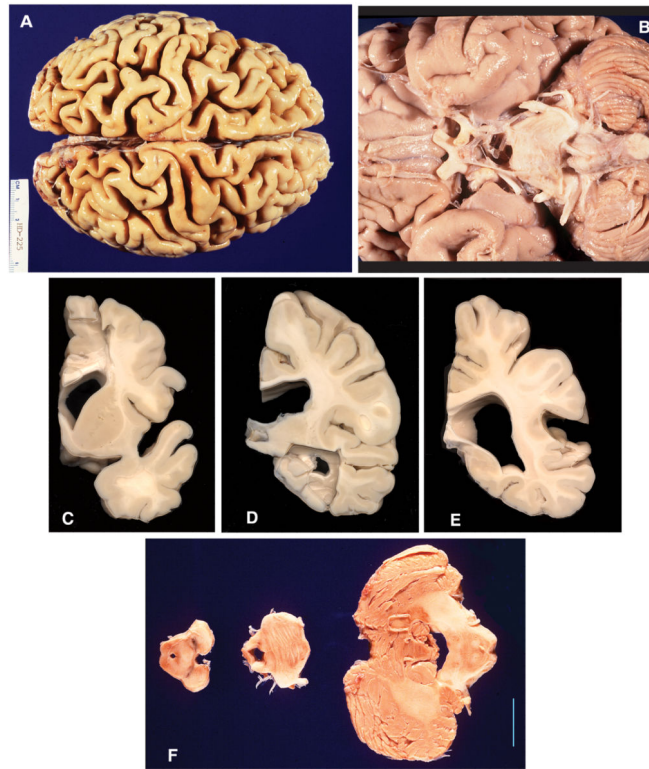
FIG. 2.
SCA12 gross neuropathology. (A) Dorsal view of cerebral hemispheres showing diffuse cortical atrophy with enlarged cortical fissures, greatest in the parietal and posterior frontal lobes. Scale bar = 4.3 cm. (B) Inferior view, showing mild atrophy of the pons and cerebellum. Cranial nerves are unremarkable. (C) Coronal section of forebrain, showing moderate enlargement of the lateral ventricle, atrophy of the cerebral gray and white matter, and preservation of the caudate and putamen. (D) Coronal section, showing enlarged body and temporal horn of the lateral ventricle and thinning of the corpus callosum. (E) Posterior coronal section, showing enlarged trigone of the lateral ventricle, thinning of the corpus callosum, and diffuse cortical atrophy. (F) Slices of the midbrain, showing normal-appearing SN, mild atrophy of the base of the pons, and mild cerebellar atrophy. Scale bar = 2 cm.
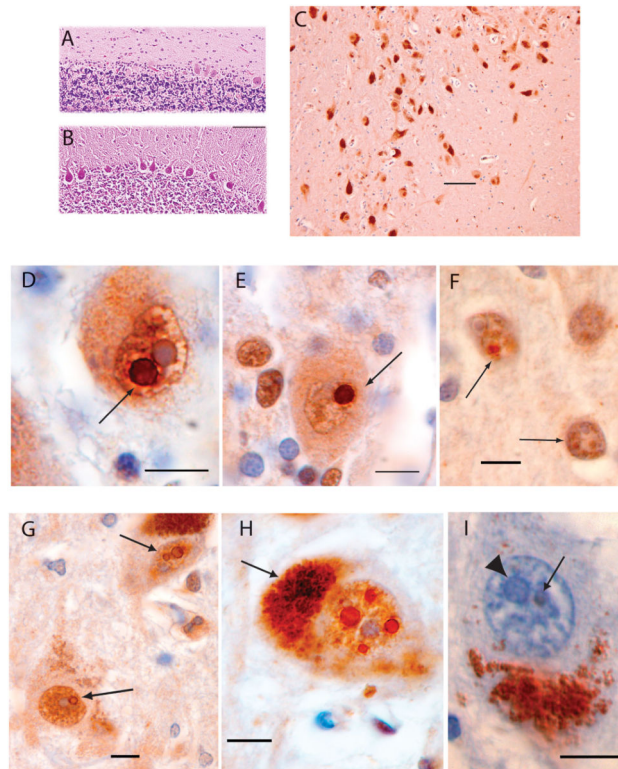
FIG. 3.

SCA12 histopathology and intranuclear neuronal inclusions. (A) SCA12 cerebellar cortex (H & E staining) showing Purkinje cell loss. (B) Cerebellar cortex, normal control: H & E staining. Scale bar = 200 μm. (C) SNpc, immunostained for ubiquitin, showing melanin-containing neurons that exhibit normal density, size, and appearance for a 66-year-old subject. Scale bar = 100 μm. (D) Purkinje cell with a ubiquitin positive, round, intranuclear inclusion (arrow) adjacent to a similarly sized pale blue nucleolus. (E) A different Purkinje cell containing a ubiquitin-positive, round, intranuclear inclusion (arrow). (F) Two neurons (arrows) in motor cortex with multiple, ubiquitin-positive, intranuclear inclusions distinct from the nucleolus (stained blue). (G) Two neurons in the SNpc. The upper neuron contains two ubiquitin-positive, intranuclear inclusions adjacent to each other and separate from the nucleolus. The lower neuron contains one ubiquitin-positive intranuclear inclusion adjacent to the nucleolus. (H) SNpc neuron with at least four round, ubiquitin-positive, intranuclear inclusions surrounding the nucleolus. Arrow points to cytoplasmic melanin. (I) SNpc neuron with cytoplasmic melanin inferiorly. Pale blue nucleolus indicated with arrowhead. Arrow points to a smaller, round inclusion that is negative for 1C2 immunostaining (expanded polyglutamine repeats) and is faintly eosinophilic. Sections D to I are immunostained for ubiquitin and counterstained with H & E. Section I is immunostained with 1C2 antibody and counterstained with H & E. Scale bars are 10 μm in sections D to I.
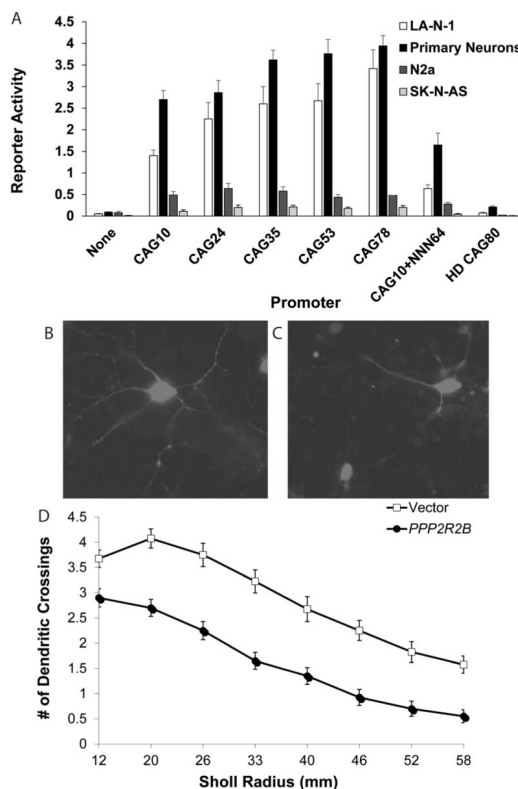
FIG. 4.

PPP2R2B promoter activity and *PPP2R2B*-induced neurotoxicity. (A) Constructs as depicted in Supporting Figure 1, with luciferase activity normalized to Renilla activity, and all values normalized to the SV40 construct (not shown on graph) to enable comparisons across experiments. This graph represents the mean and SE of five (LA-N-1 cell line and rat primary cortical neurons) or three (N2a and SK-N-AS cell lines) independent experiments, each performed in triplicate. For LA-N-1 cells, there was a strong correlation between repeat length and reporter expression ($r^2 = 0.90$; $P = 0.014$), with CAG_{10} significantly different from CAG_{35}, CAG_{53}, and CAG_{78} (ANOVA: $F = 24.51$; $P < 0.0001$; Tukey's post-hoc test: $P < 0.05$ for CAG_{35} and CAG_{53}; $P < 0.01$ for CAG_{78}). For primary rat cortical neurons, the same effect of increasing repeat length on reporter activity was evident (exponential curve: $r^2 = 0.81$; $P = 0.037$; ANOVA: $F = 58.08$; $P < 0.0001$; post-hoc Tukey's test: $P < 0.05$ for CAG_{35} and CAG_{53}; $P < 0.01$ for CAG_{78}), but no effect of repeat length was observed in N2a or SK-NAS cell lines. In LA-N-1 and rat primary cortical neurons, the reporter activity induced by the $CAG_{10}+(NNN)_{64}$ construct was equivalent to the *PPP2R2B*-CAG_{10} construct and was significantly less than activity induced by the CAG_{78} construct ($P < 0.01$). The reporter activity of the CAG80-HD construct was minimal; activity was significantly less than the CAG_{10} construct and substantially less than the CAG_{78} construct in LA-N-1 cells (post-hoc: $P < 0.05$ and $P < 0.01$, respectively) and primary rat cortical neurons ($P < 0.01$ for each comparison). (B and C) Primary cortical neurons cotransfected with DsRed and *Bβ1* variant of *PPP2R2B*, fixed at 72 hours post-transfection, 100x magnification. Neurite outgrowth is markedly greater in cells transfected with vector (B) than in cells transfected with *PPP2R2B* encoding Bβ1 (C). (D) Sholl analysis demonstrating loss of neurite

outgrowth after overexpression of PPP2R2B (ANOVA: $F = 541.5$; $P < 0.0001$). Experiment performed in triplicate; N = 25 to 40 neurons in each experiment per condition. ANOVA, analysis of variance.

TABLE 1

Gross brain pathology

Brain Region	Gross Pathological Results
Cerebral cortex	Atrophic gyri and widened sulci (Fig. 2A). Diffuse cortical atrophy, marked at the parietal lobes and posterior aspect of the frontal lobes (Fig. 2A). Small, symmetric, cerebral hemispheres (Fig. 2C–E). Selective thinning of the cortical gray matter well demarcated from underlying white matter. The volume of cerebral white matter was also reduced and the corpus callosum was thin (Fig. 2D), with normal myelination.
Ventricular system	Moderate hydrocephalus, more prominent in the lateral ventricles.
Hippocampus	Mild atrophy accompanied by widening of the temporal horns of the lateral ventricles.
Thalamus and hypothalamus	Proportionate to the size of the brain, but the medial walls appeared concave in association with a dilated third ventricle. Subthalamic region was normal.
Other cortical regions	The amygdalae and entorhinal cortices appeared normal. The caudate and putamen were of normal shape and their size was proportional to that of the brain.
Midbrain and medulla	Midbrain and medulla were slightly atrophic, but proportional to the size of the brain (Fig. 2F). The midbrain showed mild atrophy, but the substantia nigra (SN) was well pigmented. Cerebral peduncles were normal.
Pons	Mildly atrophic and the basis pontis was scalloped with mild atrophy (Fig. 2B,F). The tegmentum appeared normal and the locus ceruleus was normally pigmented.
Cranial nerves	Cranial nerves were unremarkable (Fig. 2B).
Cerebellum	Mildly decreased in size. The deep nuclei and white matter were normal. The cerebellar folia, however, showed mild atrophy manifest by subtle widening of the sulci (Fig. 2F).
Other gross findings	At autopsy, body weight was 44.2 kg and body length was 160 cm. Brain weight was 1,045 g (normal, 1,300–1,400 g). The cranial cavity was normal. The brain was covered with translucent meninges. Mild,nonocclusive, atherosclerotic plaques were present in the proximal portions of both middle cerebral arteries. The spinal cord was not recovered.